

Rotor Position Estimation of Permanent Magnet Synchronous Motor Based on Disturbance Model

Qiang MEN, Jiaming CAI¹, Junbi TAN and Xiangtao FANG
Shenzhen Topband Company Limited, Shenzhen 518000, China

Abstract. Aiming at the high reliability of sensorless control of permanent magnet synchronous motor (PMSM), a back EMF estimator based on disturbance model is proposed. The back EMF in the assumed coordinate system is taken as the disturbance item of slow change, and the motor disturbance observation model is established. According to the characteristics of the observed back EMF, a phase-locked loop is designed to estimate the rotor speed and position. Through the analysis of the software simulation and physical verification results of the control model, it is proved that the observer model has high stability and adaptability for the estimation of the high and low speed operation region of the motor.

Keywords. Sensorless, assumed coordinate system, disturbance observer

1. Introduction

PMSM has many advantages, such as high power density, small size, high efficiency, good controllability and so on, while reducing the system cost. With the improvement of its performance, more and more application fields will transition from sensor control system to sensorless control system [1]. The sliding mode observer scheme mentioned in literature [2, 3] is severely limited in the application of ultra-low speed and ultra-high speed because the effective back EMF signal needs to be extracted from the high-frequency switching signal with a large number of harmonic signals. The high-frequency voltage injection method proposed in [4, 5] is only applicable to the low-speed operation of the motor, and requires additional high-frequency excitation voltage, which will produce a certain electromagnetic noise power loss [4, 5]. The flux estimation method proposed in literature [6] can significantly reduce the minimum operating speed of the motor, but it is sensitive to the flux parameters [6].

To solve the above problems, this paper proposes an observer with good adaptability to high and low speeds, and does not need the flux parameters of the motor. According to the PMSM voltage model in the assumed coordinate system ($\gamma\delta$) and the motor resistance and inductance parameters measured offline, the disturbance observation model is established with the $\gamma\delta$ -axis back EMF as the slowly varying disturbance term. The back EMF of the γ -axis includes the estimated angle error $\Delta\theta$. Therefore, it is necessary to design a phase-locked loop to eliminate the

¹ Corresponding author, Jiaming Cai, Shenzhen Topband Company Limited, Topband Industrial Park, Tangtou Community, Shiyuan Street, Shenzhen 518000, China; E-mail: 977540122@qq.com.

estimated rotor position error until the estimated rotor position converges correctly. The observer model is simple in design, has excellent transient and steady-state characteristics, does not need to compensate the observation angle hysteresis in the full speed domain, and is robust to the variation of motor parameters.

2. Assumed Rotating Coordinate System

An assumed rotating coordinate system $\gamma\delta$ is defined, and the relationship between the assumed coordinate system $\gamma\delta$ and the actual rotor coordinate system dq is shown in Figure 1. The α -axis of the $\alpha\beta$ coordinate system coincides with the A-phase axis of the ABC coordinate system, they are stationary relative to the motor stator. dq is the rotor coordinate system, and now define, the Angle between the d axis and the A axis is θ , and the rotational angular velocity is ω_e . Assumed rotating coordinate system $\gamma\delta$ rotates with angular velocity $\hat{\omega}_e$, and that the γ axis is ahead of the d axis by an angle $\Delta\theta$.

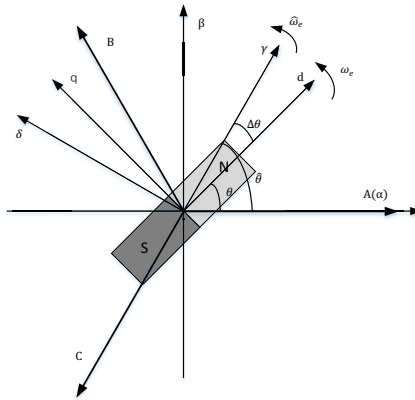


Figure 1. Schematic diagram of multi coordinate system.

2.1. Voltage Equation In $\gamma\delta$ Coordinates

Ignored the hysteresis, eddy current loss, and the resistance, inductance, flux and other time-varying nonlinear factors of the motor, and the magnetic field is considered to be uniformly distributed in the air gap with sinusoidal characteristics. Then the voltage equation of the Surface permanent magnet synchronous motor in the two-phase stationary coordinate system ($\alpha\beta$) is:

$$\begin{cases} u_\alpha = Ri_\alpha + L_s \frac{di_\alpha}{dt} - \omega_e \varphi_d \sin \theta \\ u_\beta = Ri_\beta + L_s \frac{di_\beta}{dt} + \omega_e \varphi_d \cos \theta \end{cases} \quad (1)$$

Where, u_α , u_β , i_α , i_β are the voltage and current components of $\alpha\beta$ axis respectively, R is the stator resistance, L_s is the stator inductance, φ_d is the rotor flux, ω_e is the rotor angular velocity, θ is rotor Angle, the α axis overlapped with the A axis in Figure 1, and the β axis was 90° ahead of the α axis counterclockwise.

According to Figure 1, that the voltage equation in the assumed coordinate system ($\gamma\delta$) can be obtained by multiplying the voltage equation in the stationary coordinate system ($\alpha\beta$) by the rotation matrix $T(\hat{\theta})$.

$$T(\hat{\theta}) = \begin{pmatrix} \cos \hat{\theta} & \sin \hat{\theta} \\ -\sin \hat{\theta} & \cos \hat{\theta} \end{pmatrix} \tag{2}$$

Where, $\hat{\theta}$ is the Angle between the γ axis and the α axis.

The voltage equation of (1) was transformed by rotation matrix $T(\hat{\theta})$, and we can obtained the voltage equation in $\gamma\delta$ coordinate system as follow:

$$\begin{bmatrix} V_\gamma \\ V_\delta \end{bmatrix} = \begin{bmatrix} R + pL_s & -\hat{\omega}_e L_s \\ \hat{\omega}_e L_s & R + pL_s \end{bmatrix} \begin{bmatrix} i_\gamma \\ i_\delta \end{bmatrix} + \begin{bmatrix} e_\gamma \\ e_\delta \end{bmatrix} \tag{3}$$

Where, V_γ , V_δ , i_γ , i_δ are the voltage and current components of $\gamma\delta$ axis respectively. p is the differential operator, ω_e and $\hat{\omega}_e$ represent the rotational angular velocities of the dq and $\gamma\delta$ coordinates, respectively. $\begin{bmatrix} e_\gamma \\ e_\delta \end{bmatrix} = \omega_e \varphi_d * \begin{bmatrix} \sin \Delta\theta \\ \cos \Delta\theta \end{bmatrix}$, Where, $\Delta\theta = \hat{\theta} - \theta$. It can be seen that e_γ and e_δ contain the real rotor position information θ , so we need to estimate e_γ and e_δ first.

From the voltage equation in equation (3) above, it can be seen that the voltage equation in $\gamma\delta$ coordinate system includes input variables V_γ and V_δ , state variables i_γ and i_δ , Cross coupling term $-\hat{\omega}_e L_s i_\delta$ and $\hat{\omega}_e L_s i_\gamma$, the back electromotive force term e_γ and e_δ . In most of the fan, pump control applications. The change in mechanical speed is relatively slow and can be considered to be well below the sampling and execution frequency of electrical systems, Therefore, e_γ and e_δ can be approximated as constant disturbance inputs. Since the disturbance input contains the rotor position estimation error information, we need to design a disturbance observer to estimate the disturbance term in real time, and then use PLL to make the rotor error approach zero, at which time the estimated rotor position converges to the real rotor position.

2.2. Design of Disturbance Observer in Assumed Coordinate System

Selecting i_γ , i_δ , e_γ , and e_δ as state variables, the voltage equation of equation (3) is rewritten in the form of state equation. Since the mechanical time constant of the motor system is much larger than the electrical time constant, the rotational speed can be approximated as a constant value in the electrical cycle, i.e., $\frac{d}{dt} e_\gamma \approx 0, \frac{d}{dt} e_\delta \approx 0$. The following state equation can be obtained

$$\begin{cases} \frac{d}{dt} i_\gamma = \frac{1}{L_s} [V_\gamma - R i_\gamma + L_s \hat{\omega}_r i_\delta - e_\gamma] \\ \frac{d}{dt} i_\delta = \frac{1}{L_s} [V_\delta - R i_\delta - L_s \hat{\omega}_r i_\gamma - e_\delta] \\ \frac{d}{dt} e_\gamma = 0 \\ \frac{d}{dt} e_\delta = 0 \end{cases} \tag{4}$$

Based on the electrical model (4), we propose the following observer of the electrical system [6]:

$$\begin{cases} \frac{d}{dt} \hat{i}_\gamma = \frac{1}{L_s} [V_\gamma - R\hat{i}_\gamma + L_s \hat{\omega}_r i_\delta - \hat{e}_\gamma + k_1 \tilde{i}_\gamma] \\ \frac{d}{dt} \hat{i}_\delta = \frac{1}{L_s} [V_\delta - R\hat{i}_\delta - L_s \hat{\omega}_r i_\gamma - \hat{e}_\delta + k_2 \tilde{i}_\delta] \\ \frac{d}{dt} \hat{e}_\gamma = k_3 \tilde{i}_\gamma \\ \frac{d}{dt} \hat{e}_\delta = k_4 \tilde{i}_\delta \end{cases} \tag{5}$$

Where, $\hat{i}_\gamma, \hat{i}_\delta, \hat{e}_\gamma, \hat{e}_\delta$ are the estimated current and estimated back electromotive force of the $\gamma\delta$ coordinate system, respectively. And define, the estimate current error $\tilde{i}_\gamma = \hat{i}_\gamma - i_\gamma, \tilde{i}_\delta = \hat{i}_\delta - i_\delta$, the estimate back electromotive force error $\tilde{e}_\gamma = \hat{e}_\gamma - e_\gamma, \tilde{e}_\delta = \hat{e}_\delta - e_\delta$, respectively. According to Equations (4) and (5), the state error equation can be obtained as follows:

$$\begin{pmatrix} \frac{d}{dt} \tilde{i}_\gamma \\ \frac{d}{dt} \tilde{i}_\delta \\ \frac{d}{dt} \tilde{e}_\gamma \\ \frac{d}{dt} \tilde{e}_\delta \end{pmatrix} = \mathbf{A} \begin{pmatrix} \tilde{i}_\gamma \\ \tilde{i}_\delta \\ \tilde{e}_\gamma \\ \tilde{e}_\delta \end{pmatrix} \tag{6}$$

Where, $\mathbf{A} = \begin{pmatrix} \frac{k_1-R}{L_s} & 0 & -\frac{1}{L_s} & 0 \\ 0 & \frac{k_2-R}{L_s} & 0 & -\frac{1}{L_s} \\ k_3 & 0 & 0 & 0 \\ 0 & k_4 & 0 & 0 \end{pmatrix}$

According to the system state equation matrix \mathbf{A} , the characteristic equation of \mathbf{A} is obtained as follows:

$$\det(s\mathbf{I} - \mathbf{A}) = \left(s^2 - \frac{k_2-R}{L_s} * s + \frac{k_4}{L_s}\right) * \left(s^2 - \frac{k_1-R}{L_s} * s + \frac{k_3}{L_s}\right) \tag{7}$$

Where, s is the Laplace operator; \mathbf{I} is a 4-dimensional is identity matrix.

Force the characteristic equation equal to zero, i.e. $\det(s\mathbf{I} - \mathbf{A}) = 0$, to solve the characteristic roots as follows:

$$s_{1,2} = \frac{\frac{k_2-R}{L_s} \pm \sqrt{\left(\frac{k_2-R}{L_s}\right)^2 - 4 * \frac{k_4}{L_s}}}{2}, \quad s_{3,4} = \frac{\frac{k_1-R}{L_s} \pm \sqrt{\left(\frac{k_1-R}{L_s}\right)^2 - 4 * \frac{k_3}{L_s}}}{2}$$

The stability condition of the observer system is that the characteristic roots must have negative real parts. In order to simplify the stability design of the system, the stability condition can be satisfied only when the two terms in the molecule of the

characteristic root equation $s_{1,2}$ and $s_{3,4}$ are less than zero, respectively. That is, the observer is stable when the following conditions are met:

$$\begin{cases} k_1 < R \\ k_2 < R \\ k_3 > 0 \\ k_4 > 0 \end{cases} \tag{8}$$

The pole distribution of the observer can be changed by adjusting the values of k_1 , k_2 , k_3 and k_4 on the premise of satisfying the stability, so that the observer can meet the desired performance index.

2.3. The design of Rotor Angle observer

When the \hat{e}_γ and \hat{e}_δ is accurately observed, Equation (4) shows that the estimated back electromotive force term $e_\gamma = \omega_e \varphi_d \sin(\hat{\theta} - \theta) = \omega_e \varphi_d \sin(\Delta\theta)$ in the voltage equation of the γ axis contains the angular error information $\Delta\theta$ of the $\gamma\delta$ coordinate system and the dq coordinate system. According to the principle of PLL, the above Angle error $\Delta\theta$ can be eliminated by PLL. When $\Delta\theta=0$, it means that the observed Angle and angular velocity converge to the correct rotor Angle and angular velocity.

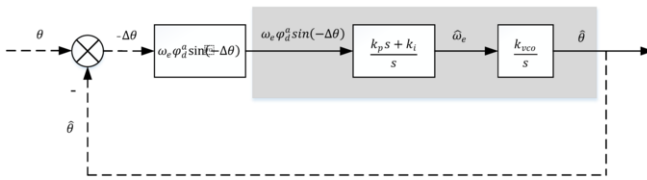


Figure 2. Phase locked loop control loop.

Figure. 2 shows the PLL control loop for observing rotor Angle and angular velocity. The shaded part of the figure is the proposed PLL structure. The input signal is the estimated back electromotive force $\hat{e}_\gamma = \omega_e \varphi_d \sin(\Delta\theta)$ on the γ axis, and the estimated angular velocity $\hat{\omega}_e$ is obtained from the active power low pass filter, and then the estimated Angle $\hat{\theta}$ is obtained from the integrator. The dotted line is an extended diagram to facilitate the overall understanding and analysis of the PLL system.

On the premise of PLL stability, small signal analysis of the system is carried out. The dynamic characteristics of the system near the stable point are analyzed. The PLL closed-loop transfer function of the loop is as follows:

$$\phi(s) = \frac{k_0 * k_{vco} * s + k_0 * k_{vco} * k_i}{s^2 + k_0 * k_{vco} * k_p * s + k_0 * k_{vco} * k_i} \tag{9}$$

Where, $k_0 = \omega_e \varphi_d$. In this paper, we only consider when w is greater than zero, so $k_0 > 0$.

With reference to the classical second-order transfer function, the damping coefficient is chosen as $\zeta = 0.707$, then the natural frequency ω_n can be designed by the desired stabilization time t_s . The calculated relation is as follows:

$$\omega_n = \frac{4}{\zeta t_s} \tag{10}$$

Where, t_s is the stabilization time.

3. Simulation and Experimental Results

3.1. Simulation Results and Analysis

In order to verify the correctness and feasibility of the proposed scheme, the above scheme is simulated in Matlab environment. A permanent magnet synchronous motor is selected, and the motor parameters are shown in Table 1.

Table 1. Parameters of permanent magnet synchronous motor.

Parameter	Value
Stator winding resistance (Ω)	2
Stator winding inductance (H)	0.0026
Pair of Poles	4
EMF constant (V·s)	0.35
Moment of inertia ($\text{kg}\cdot\text{m}^2$)	0.2621417
Moment of inertia (N·m)	2
Viscous damping (N·m·s)	0.00303448

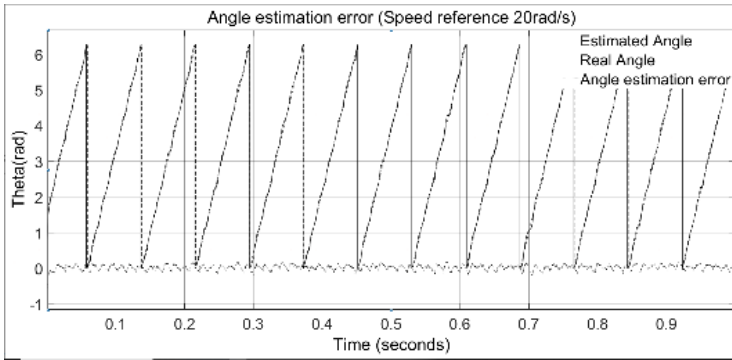


Figure 3. Estimation angle and estimation error of stable operation at 20rad/s.

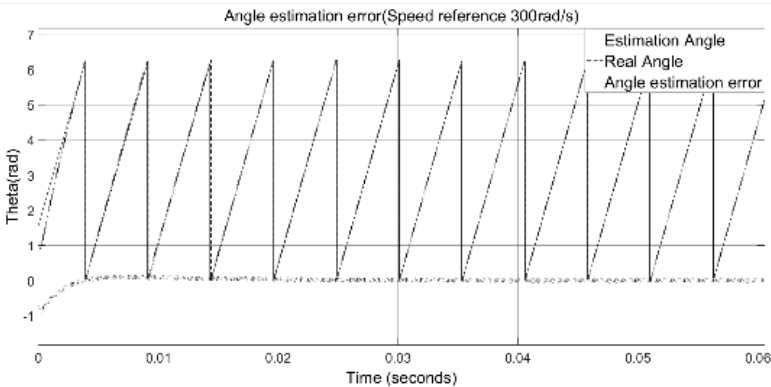


Figure 4. Estimation angle and estimation error of stable operation at 300rad/s.

When the motor is loaded with 9.2Nm and the electrical angular speed is 20rad/s, the observation angle lags behind the actual angle by a maximum of 0.5rad (Figure 3). When the electrical angular velocity is 300 rad/s, the observation angle lags behind the actual angle by 0.072 rad at most (Figure 4). It can be seen that the observer has good load operation capability and observation accuracy in high and low speed regions.

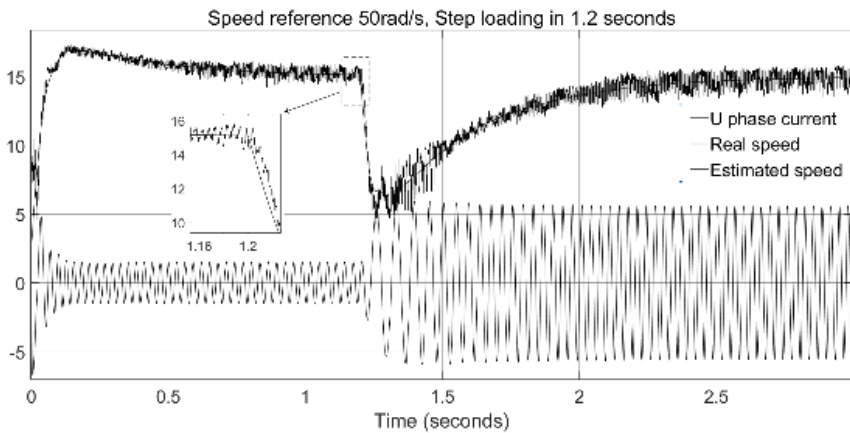


Figure 5. Operate at the target speed of 50rad/s, suddenly increase the load at 1.2s.

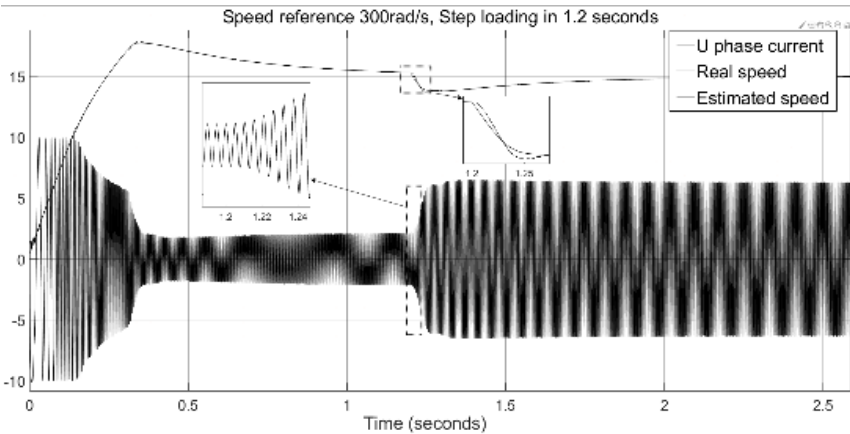


Figure 6. Operate at the target speed of 300rad/s, suddenly increase the load at 1.2s.

Figure 5 shows the phase current, actual speed (16.5rad/s/grid), and estimated speed (16.5rad/s/grid) waveforms of the whole process when the initial target angular speed of the motor is 50 rad/s and the load torque suddenly increases at 1.2s. At the moment of sudden load, the running speed of the motor decreases. The maximum decreasing speed is about 15% of the rated speed (30rad/s). The time from the moment of sudden load to the moment when the motor speed recovers to the stable running value is about 1s.

Figure 6 shows the phase current, actual speed (25rad/s/grid), and estimated speed (25rad/s/grid) waveforms of the whole process when the initial target angular speed of the motor is 200rad/s and the load torque suddenly increases at 1.2s. At the moment of sudden load application, the running speed of the motor decreases, and the maximum decreasing speed is about 10% of the rated speed (20rad/s), which causes the output

current of the controller to increase rapidly, and the final speed is stabilized within the target speed range. It takes about 0.8s from the moment of sudden load application to the time when the motor speed recovers to the stable operation value. It can be seen from the actual speed waveform and current waveform that the motor system can accurately and quickly follow the sudden change of speed caused by load changes. And it can operate stably at high speed with load.

3.2. Experimental Results and Analysis

In order to verify the feasibility and effectiveness of the above scheme, the fan in the range hood product is used as the object for the experiment. The experimental controller is GD32F330, a 32-bit chip of GD Company, and the development environment is Keil4, In the experiment, the PWM carrier frequency is 10kHz. Use the timer to output the estimated speed variable in the form of PWM duty cycle, and display it on the oscilloscope after low-pass filtering. The above scheme is used as the theoretical basis for software development and debugging. The parameters of the permanent magnet synchronous motor used in the experiment are the same as those in Table 1.

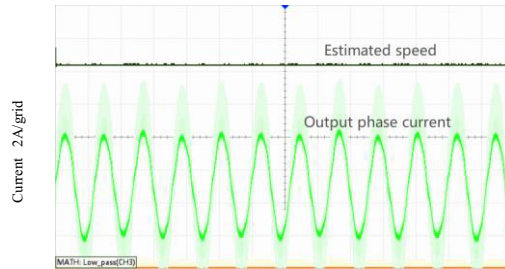


Figure 7. Speed and current during 2500r/min stable operation(5ms/grid)

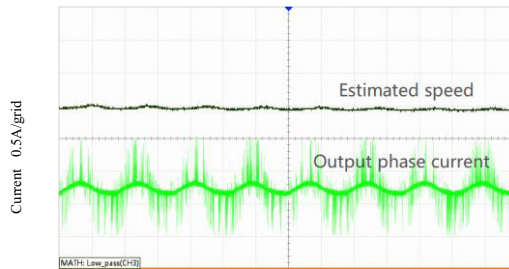


Figure 8. Speed and current during 160r/min stable operation(50ms/grid)

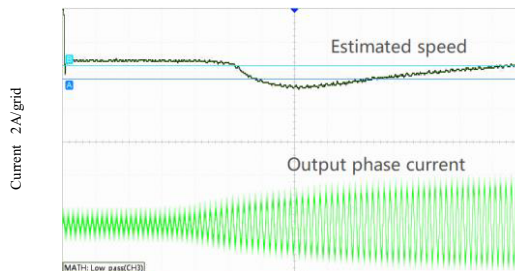


Figure 9. Speed and current after sudden load during 2500r/min stable operation(100ms/grid)

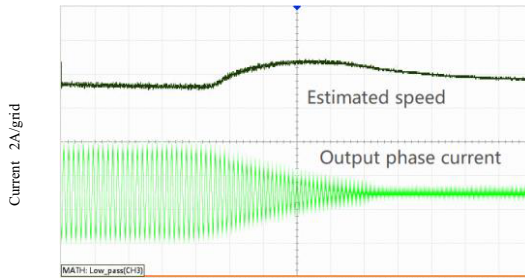


Figure 10. Speed and current after sudden load reduction during 2500r/min stable operation(100ms/grid)

Figure 7 and 8 correspond to the current/speed waveforms of the fan at high speed and low speed respectively. The overall speed output is stable, and the current waveform is free of jitter and distortion. At low speed, the estimated speed fluctuates slightly, but the fluctuation is small. The experiment shows that the fan has good running stability and strong carrying capacity at a given speed of 2500r/min and 160r/min.

In order to verify the speed response capability of the fan when it runs at high speed with load, the sudden load increase/decrease test is conducted when the motor runs at 2500 rpm at high speed. It can be seen from Figure 9 that after the sudden load increase, the fan's running speed decreases, with the maximum decreasing speed of about 410 rpm and the recovery time of 0.9s; In Figure 10, after the sudden load reduction, the operating speed of the fan increases, the maximum speed is about 350 rpm, and the recovery time is 1.2s. The experiment shows that the output current responds quickly and stably before and after the load changes, without sudden change or fluctuation, and the motor operates stably and reliably.

4. Conclusion

In this paper, the principle of the position observer of PMSM based on the assumed coordinate system is analyzed. Compared with the observer designed in the traditional static coordinate system, the observer is a constant when the system is in steady state, and there is no phase delay caused by filtering effect in the steady-state angle estimation. At the same time, the parameter design of the observer is simpler and the performance is better. In addition, the design of the observer does not require the constant term of the back EMF, and it has strong robustness to the flux change during the operation of the motor. The experimental results show that the scheme can effectively observe the speed and position of the PMSM in real time at medium and high speeds, and has high estimation accuracy and anti load disturbance ability for speed and position.

References

- [1] Sul SK, Kwon YC, Lee Y. Sensorless control of IPMSM for last 10 years and next 5 years. *CES Transactions on Electrical Machines & Systems*. 2017, 1(2):91-99.

- [2] Lu WQ, Hu YW, Du XY, Huang WX. Sensorless vector control speed regulation system with new sliding mode observer for permanent magnet synchronous motor. *Chinese Journal of Electrical Engineering*. 2010;30(33):78-83.
- [3] Li R, Zhao GZ, Xu SJ. Sensorless control of permanent magnet synchronous motor based on extended sliding mode observer. *Journal of Electrical Technology*. 2012;27(03):79-85.
- [4] Liu Y, Zhou B, Feng Y, Zhao CL. Low speed sensorless control and position estimation error compensation of permanent magnet synchronous motor. *Journal of Electrical Technology*. 2012;27(11):38-45.
- [5] Kim S, Ha J and Sul S. PWM Switching Frequency Signal Injection Sensorless Method in IPMSM. *IEEE Transactions on Industry Applications*. 2012; 48(5): 1576-1587.
- [6] Ortega R, Praly L, Astolfi A, Lee J and Nam K. Estimation of rotor position and speed of permanent magnet synchronous motors with guaranteed stability. *IEEE Transactions on Control Systems Technology*. 2011; 19(3):601-614.